

Structure of the Pore-forming Transmembrane Domain of a Ligand-gated Ion Channel*

Received for publication, March 8, 2001, and in revised form, April 26, 2001
Published, JBC Papers in Press, April 27, 2001, DOI 10.1074/jbc.M102101200

Nathalie Méthot‡, Blair D. Ritchie‡, Michael P. Blanton§, and John E. Baenziger‡||

From the ‡Department of Biochemistry, Microbiology, and Immunology, University of Ottawa, Ottawa, Ontario, K1H 8M5, Canada and §Departments of Anesthesiology and Pharmacology, Texas Tech University Health Sciences Center, Lubbock, Texas 79430

The structure of the pore-forming transmembrane domain of the nicotinic acetylcholine receptor from *Torpedo* has been investigated by infrared spectroscopy. Treatment of affinity-purified receptor with either Pronase or proteinase K digests the extramembranous domains (roughly 75% of the protein mass), leaving hydrophobic membrane-imbedded peptides 3–6 kDa in size that are resistant to peptide $^1\text{H}/^2\text{H}$ exchange. Infrared spectra of the transmembrane domain preparations exhibit relatively sharp and symmetric amide I and amide II band contours centered near 1655 and 1545 cm^{-1} , respectively, in both $^1\text{H}_2\text{O}$ and $^2\text{H}_2\text{O}$. The amide I band is very similar to the amide I bands observed in the spectra of α -helical proteins, such as myoglobin and bacteriorhodopsin, that lack β structure and exhibit much less β -sheet character than is observed in proteins with as little as 20% β sheet. Curve-fitting estimates 75–80% α -helical character, with the remaining peptides likely adopting extended and/or turn structures at the bilayer surface. Infrared dichroism spectra are consistent with transmembrane α -helices oriented perpendicular to the bilayer surface. The evidence strongly suggests that the transmembrane domain of the nicotinic receptor, the most intensively studied ligand-gated ion channel, is composed of five bundles of four transmembrane α -helices.

The nicotinic acetylcholine receptor (nAChR)¹ from *Torpedo* is an abundant neurotransmitter-gated ion channel that is used extensively as a structural model for homologous ligand-gated channels located throughout the central and peripheral nervous systems (1–4). The nAChR is composed of four subunits organized pseudo-symmetrically as an $\alpha_2\beta\gamma\delta$ pentamer around a central ion channel pore. The ion channel transiently gates open in response to the binding of two molecules of acetylcholine, leading to the flux of cations across the postsynaptic membrane. Prolonged exposure to acetylcholine converts the nAChR into a nonconducting desensitized state. Each of the

four subunits contains a large extracellular N-terminal domain, four 25–30-amino acid-long hydrophobic segments designated M1 to M4, and a cytoplasmic loop between the M3 and M4 transmembrane segments. The N-terminal domain of each α -subunit contains one binding site for acetylcholine. The four transmembrane segments form the ion channel pore, with M2 from each subunit directly lining the ion channel. The intracellular loop between M3 and M4 may serve as a regulatory domain in that several residues can be phosphorylated, leading to altered rates of desensitization.

The structure of the transmembrane domain of the nAChR has been the subject of considerable recent investigation. All four transmembrane segments were originally assigned α -helical secondary structures based on hydrophobicity analysis (5, 6). The resulting four-transmembrane- α -helices-per-subunit model is supported by a large body of biochemical and biophysical data, including the α -helical-labeling pattern of the exposed transmembrane surfaces by both ion channel-specific and lipid-soluble photoactivatable probes (7–10), the predominantly α -helical secondary structure of the exchange-resistant and likely integral membrane “core” nAChR peptide hydrogens (11, 12), and the predominantly α -helical secondary structures of isolated and reconstituted transmembrane segments (13–16). A 9 Å resolution structure of the nAChR exhibits five rods of electron density lining the ion channel pore, consistent with α -helical transmembrane M2 pore-lining segments (17). In contrast, the cryoelectron microscopic studies reveal a diffuse pattern of electron density at the periphery of the receptor transmembrane domain that has been interpreted in terms of M1, M3, and M4 from each subunit, contributing to a ring of transmembrane β -strands surrounding an inner core of channel-lining M2 α -helices (17). FTIR studies of proteolytically degraded native nAChR membranes and molecular modeling are both consistent with a mixture of α -helices and β -strands forming the transmembrane domain (18–20). A mixed secondary structure has also been suggested for the transmembrane domain of the glycine receptor (21, 22).

The mixed α -helix/ β -sheet structure suggested by Unwin (17) represents a new motif for the transmembrane domains of integral membrane proteins in general and for neurotransmitter-gated ion channels in particular. The proposed transmembrane structure has important implications for the mechanisms of channel gating and desensitization as well as for the mechanisms of channel regulation by endogenous factors such as receptor phosphorylation. The transmembrane model also questions the general validity of interpreting hydrophobicity plots in terms of transmembrane α -helices.

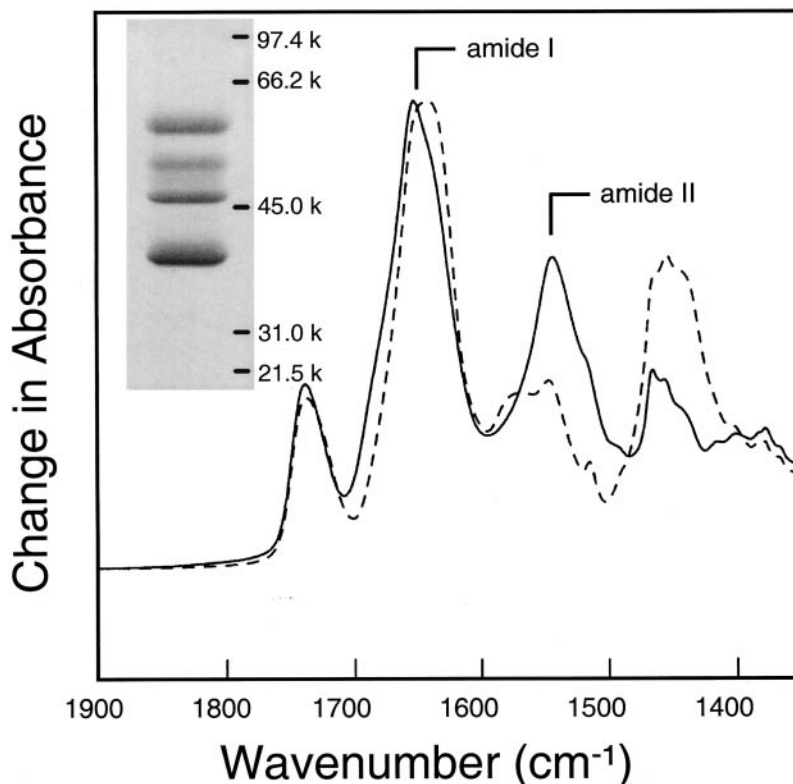
Here, we examine the secondary structure of the transmembrane domain of affinity-purified nAChR. In contrast to recent proteolytic studies on native membranes (18), our analysis shows that all nAChR transmembrane segments adopt α -heli-

* This work was supported in part by a grant from the Canadian Institutes of Health Research (to J. E. B.) and National Institutes of Health Grant NS35786 (NINDS) (to M. P. B.). The costs of publication of this article were defrayed in part by the payment of page charges. This article must therefore be hereby marked “advertisement” in accordance with 18 U.S.C. Section 1734 solely to indicate this fact.

|| To whom correspondence should be addressed: Dept. of Biochemistry, Microbiology, and Immunology, University of Ottawa, 451 Smyth Rd., Ottawa, ON, Canada K1H 8M5. Tel.: 613-562-5800 (ext. 8222); Fax: 613-562-5440; E-mail: jebaenz@uottawa.ca

¹ The abbreviations used are: nAChR, nicotinic acetylcholine receptor; FTIR, Fourier transform infrared; [¹²⁵I]TID, 3-(trifluoromethyl)-3-*m*-(¹²⁵I)iodophenyl)diazirine; *R*, dichroic ratio; PAGE, polyacrylamide gel electrophoresis; Tricine, *N*-[2-hydroxy-1,1-bis(hydroxymethyl)ethyl]glycine.

FIG. 1. FTIR spectra of intact affinity-purified nAChR recorded using the attenuated total reflection technique in both $^1\text{H}_2\text{O}$ (solid line) and $^2\text{H}_2\text{O}$ (dashed line). Inset, 10% SDS-PAGE of intact affinity-purified nAChR. *k*, kilodalton.



cal secondary structures. Our results strongly support an nAChR transmembrane domain composed of five bundles of four-transmembrane α -helices.

EXPERIMENTAL PROCEDURES

Sample Preparation—The nAChR from frozen *Torpedo californica* electric tissue (Marinus, Inc., Long Beach, CA) was affinity-purified on a bromoacetylcholine bromide-derivatized Bio-Rad Affi-Gel 201 column and reconstituted into membranes composed of 3:1:1 egg phosphatidylcholine/dioleoylphosphatidic acid/cholesterol (23). This lipid composition supports both cation flux and agonist-induced conformational change. Affinity-purified membranes typically give a purity of 90–100% nAChR, as estimated by [^{125}I]-bungarotoxin binding (24) (see also the inset of Fig. 1).

Proteolytic Treatment—Proteinase K treatment was essentially as described previously for native nAChR membranes (18), except that the affinity-purified nAChR membranes were dissolved in a solution containing 5 mg/ml proteinase K, 50 mM phosphate buffer, and 150 mM KCl at pH 8.0. Samples were incubated at 37 °C for 24 h, and equivalent aliquots of proteinase K were added after 3 and 7 h. Before digestion with Pronase, the nAChR membranes were permeabilized with saponin to ensure enzyme access to both faces of the nAChR membranes. The nAChR was suspended at a concentration of 5 mg/ml in 2 mM phosphate buffer, pH 8.0. A small volume containing 0.01 mg/ml saponin in 2 mM phosphate buffer was added to give a final saponin concentration of 0.5 $\mu\text{g}/\text{ml}$. After incubation overnight at 4 °C, the nAChR was centrifuged for 30 min, the resulting pellets dissolved in a 0.2 mg/ml Pronase solution containing 0.1 M Tris and 10 mM CaCl_2 at pH 7.5, and the nAChR membranes were incubated at 37 °C for 24 h. Both reactions were stopped with the addition of phenylmethylsulfonyl fluoride to a final concentration of 5 mM. An equal volume of 1 M NaCl was added, each tube was shaken on ice for 1 h to solubilize any aggregated peptides, and the membranes were pelleted 2 times to isolate the integral membrane peptides. The final pellets were resuspended in 2 mM phosphate buffer and stored at -80 °C.

SDS-PAGE—Proteolytic digestion of the nAChR was assessed by Tricine SDS-PAGE on 16% gels (25) with Coomassie Blue-staining. Alternatively, the degraded nAChR was equilibrated for 1 h with 0.4 μM 3-trifluoromethyl-3-(*m*-[^{125}I]iodophenyl)diazirine [^{125}I]TID, irradiated at 365 nm for 7 min, and then run on Tricine SDS gels. Dried gels were subjected to autoradiography for 2 h with an intensifying screen.

FTIR Spectroscopy—FTIR spectra of the native and digested nAChR membranes were recorded using the attenuated total reflection technique

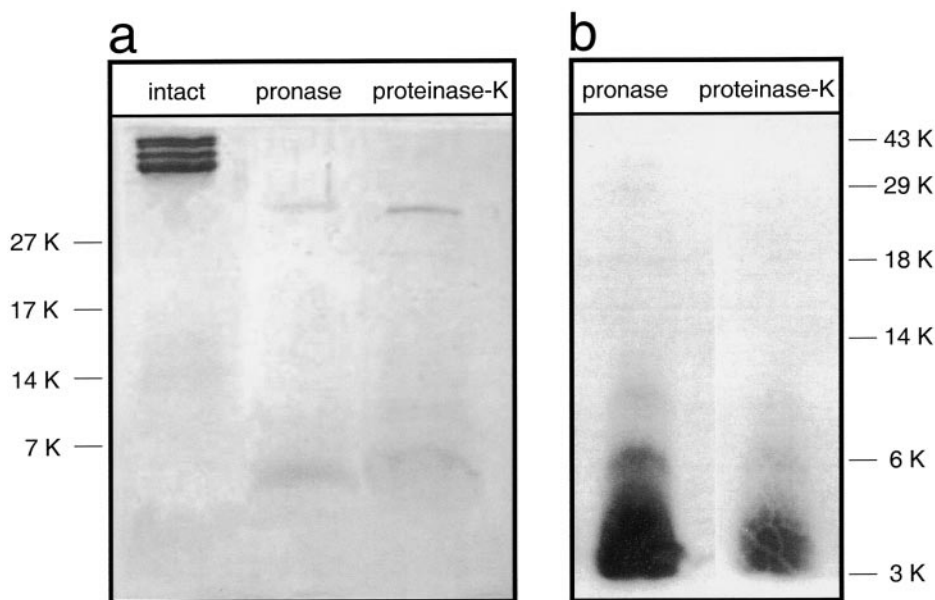
on an FTS-575 spectrometer (Bio-Rad) equipped with a DTGS detector. A small volume of nAChR containing the equivalent of 250 μg of starting material was spread on the surface of a germanium internal reflection element, and the bulk aqueous solvent was evaporated with a gentle stream of N_2 gas. The nAChR membranes were exposed to $^2\text{H}_2\text{O}$ -saturated N_2 gas for 2 h before recording spectra in the deuterated state. Each spectrum is a minimum of 256 scans, and each was recorded at 2 cm^{-1} resolution. Spectra of myoglobin, lysozyme, and trypsinogen for resolution enhancement were recorded as described elsewhere (24).

Linear Dichroism Measurements—Linear dichroism spectra were recorded in $^2\text{H}_2\text{O}$ using a Brewster angle polarizer (Harrick). Spectra were recorded with the infrared light polarized either parallel (A_{\parallel}) or perpendicular (A_{\perp}) to the plane of incidence. The dichroic ratio, R , is defined as the ratio of the absorbance of light oriented parallel (A_{\parallel}) versus perpendicular (A_{\perp}) to the plane of incidence with the germanium internal reflection element (26, 27). The thick film approximation was used to interpret the data, as samples containing similar amounts of intact nAChR are well beyond the penetration depth of the evanescent wave and saturate the absorption signal. In this approximation, an R value of 2 is defined as $R_{\text{isotropic}}$ and usually corresponds to no orientation preference. For the amide I and amide II vibrations, R values greater and less than R_{iso} , respectively, suggest a net orientation perpendicular to the internal reflection element and, thus, bilayer surface. The orientation of the transmembrane α -helices was calculated according to Hübner and Mantsch (27) from the amide II vibration dichroism assuming an angle between the amide II transition dipole and α -helix long axis of either 75 or 90°. The residual amide II band in $^2\text{H}_2\text{O}$ reflects unexchanged peptide hydrogens that are likely located within the transmembrane domain, whereas the amide I vibration likely has additional contributions from randomly oriented extended or loop structures located at the membrane surface.

RESULTS

Intact nAChR—Infrared spectra of intact affinity-purified nAChR exhibit two relatively intense protein vibrations located in the 1600–1700- cm^{-1} (amide I) and 1520–1580- cm^{-1} (amide II) regions. The amide I contour in FTIR spectra recorded in $^2\text{H}_2\text{O}$ (Fig. 1) is relatively broad and symmetric, with substantial intensity centered near both 1655 and 1635 cm^{-1} , frequencies characteristic of the α -helix and β -sheet, respectively (28–30). Both the amide I band shape and a more extensive curve-fitting

FIG. 2. Tricine SDS-PAGE of Pronase and proteinase K-degraded nAChR membranes. *a*, affinity-purified *Torpedo* nAChR membranes either before (first lane) or after proteolysis with either Pronase (second lane) or proteinase K (third lane). The gels were stained with Coomassie Blue. 15 μg of nAChR protein was loaded in the first lane. 40 μg of pre-digested nAChR was loaded in the second and third lanes. The weak band near 34 kDa was observed in all proteinase K digests and has the same migration as a proteinase K standard. *b*, the nAChR membranes degraded with Pronase (first lane) and proteinase K (second lane) were equilibrated (2 h) with [^{125}I]TID (0.4 μM) and irradiated at 365 nm for 7 min. After resolution of the polypeptides by SDS-PAGE, the gels were subjected to autoradiography. [^{125}I]TID-labeled lipid and free photolysis products were electrophoresed from the gel with the tracking dye. *k*, kilodalton.



analysis of the amide I contour suggest a mixed α -helix/ β -sheet protein with a slight predominance of α -helical secondary structures (24, 31). The secondary structure estimated for intact affinity-purified nAChR is $\sim 40\%$ α -helix and $\sim 35\%$ β -sheet, similar to values that have been reported for the nAChR based on studies of native alkaline-extracted nAChR membranes (32). The rapid (within seconds) change in amide I band shape upon exposure to $^2\text{H}_2\text{O}$ suggests the presence of a substantial number of peptides forming random conformations (11).

nAChR Transmembrane Domain—To investigate the structure of the pore-forming domain of the nAChR, the transmembrane structure was isolated by digesting the extramembranous domains with one of two water-soluble proteolytic enzymes, proteinase K or Pronase. SDS-PAGE of the transmembrane polypeptides obtained after centrifugation shows that both enzymes cleave the α , β , γ , and δ subunits, disrupting agonist binding capabilities (Fig. 2*a*). Only very weak staining near 34 kDa for the proteinase K-treated sample and potential staining below 7 kDa in both the proteinase K- and Pronase-treated samples, however, were consistently observed. The former is likely due to small amounts of proteinase K that cosediments with the nAChR membranes (see the legend to Fig. 2), whereas the latter is likely due to the proteolytically generated polypeptides (see Fig. 2*b*). The poor staining could reflect the preference of Coomassie Blue for positively charged residues and, thus, a limited ability to interact with hydrophobic transmembrane segments. This interpretation is consistent with the lack of staining observed for peptides generated in proteolytic studies of native nAChR membranes (18).

The transmembrane domain preparation was analyzed further by first photolabeling the lipid-exposed segments with the hydrophobic photoreagent [^{125}I]TID (8, 33) and then separating the labeled polypeptides by Tricine SDS-PAGE (25). As is evident in the autoradiographs of dried Tricine gels for proteinase K- and Pronase-degraded nAChRs (Fig. 2*b*), the vast majority of the [^{125}I]TID labeling is clearly detected in polypeptides migrating with apparent masses in the 3–6 kDa range. Even with a 4-fold increase in autoradiographic exposure (not shown), there is no visual evidence of [^{125}I]TID-labeled intact nAChR subunits and only very minor evidence of labeled fragments migrating with masses greater than 6 kDa. Furthermore, densitometric analysis of the autoradiographs and γ -counting of excised gel slices reveals that greater than 95% of the total [^{125}I]TID photoincorporation is restricted to peptides

in the 3–6-kDa mass range. These results indicate that the nAChR transmembrane domain preparation is comprised predominantly of polypeptides ~ 3 –6 kDa in mass, consistent with the expected mass of polypeptides containing only the nAChR transmembrane segments (5, 18, 34). N-terminal sequencing of the ^{125}I -labeled fragments confirms this result. For example, sequence analysis of the ~ 6 -kDa fragment revealed a primary peptide beginning at αMet^{243} , consistent with the presence of a peptide comprising the M2-M3 hydrophobic segments. The intense labeling with the hydrophobic reagent, [^{125}I]TID, is also consistent with a transmembrane location for the generated polypeptides.

FTIR Spectra of the nAChR Transmembrane Domain—FTIR spectra of proteolytically treated nAChR exhibit several features consistent with enzymatic digestion of the extramembranous domains (Fig. 3, *top two traces* in *a* and *b*). The intensity ratio of the 1740 cm^{-1} (lipid carbonyl stretching) to 1655 cm^{-1} (protein amide I) vibrations, which is related to lipid-protein ratio (35), increases substantially upon proteolytic treatment. The magnitude of the relative increase in intensity near 1740 cm^{-1} suggests that roughly 70% of the nAChR protein mass has been degraded, consistent with the 70–75% nAChR protein mass located outside the lipid bilayer (17, 18). There is also a dramatic loss in the intensities of bands near 1580 cm^{-1} , which are due to the vibrations of ionized carboxyl groups of aspartate and glutamate side chains (Fig. 3*b*). The loss of intensity in this region suggests that proteolytic treatment removes the vast majority of negatively charged amino acid side chains located in extramembranous regions of the nAChR. The very weak intensity remaining near 1580 cm^{-1} in the proteinase K-treated sample spectra could be due to residual proteinase K.

The proteolytically treated nAChR is relatively resistant to peptide $^1\text{H}/^2\text{H}$ exchange. Comparison of the amide II band intensities near 1547 cm^{-1} observed before and after exposure to $^2\text{H}_2\text{O}$ suggests that roughly 60% of the polypeptides generated by proteinase K treatment remain in a protiated form after 2 h of exposure to $^2\text{H}_2\text{O}$. This contrasts the roughly 90% peptide $^1\text{H}/^2\text{H}$ exchange that occurred upon exposure of three water-soluble proteins, myoglobin, lysozyme, and trypsinogen, to $^2\text{H}_2\text{O}$ for 2 h under the same experimental conditions (data not shown). The strong protection of these peptide hydrogens located in relatively short polypeptide segments to exchange with deuterium supports a location within the hydrophobic, relatively water-inaccessible environment of the lipid bilayer.

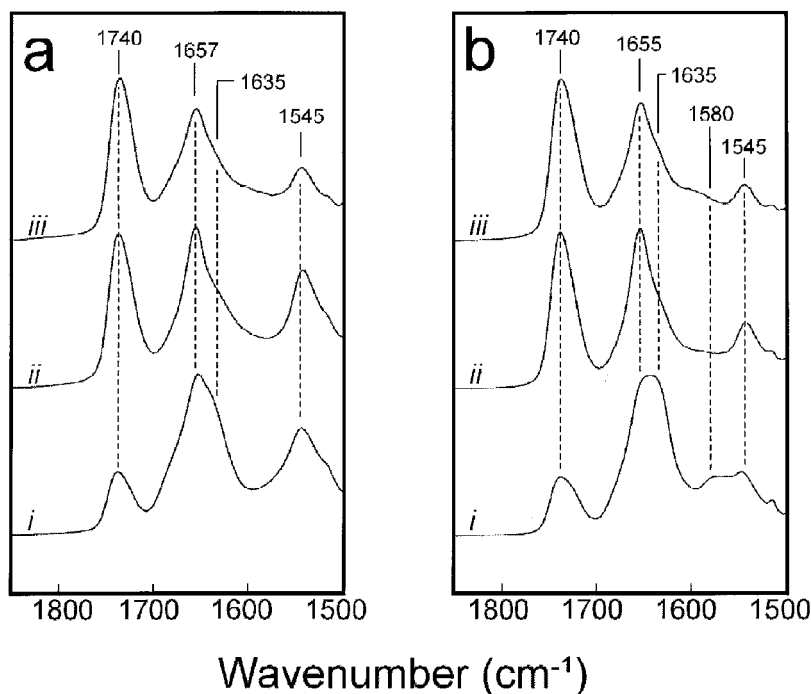


FIG. 3. FTIR spectra of intact affinity-purified nAChR and the transmembrane domain. Shown is intact affinity-purified nAChR (*i*), Pronase-treated nAChR (*ii*), and proteinase K-treated nAChR (*iii*), recorded in either $^1\text{H}_2\text{O}$ (*a*) or $^2\text{H}_2\text{O}$ (*b*).

Pronase-treated nAChR is also resistant to peptide $^1\text{H}/^2\text{H}$ exchange (40–50% protiated after 2 h), but prior permeabilization of the membranes with saponin slightly enhances peptide $^1\text{H}/^2\text{H}$ exchange rates relative to the proteinase K-treated receptor.

Secondary Structure of the Transmembrane Domain—In contrast to spectra of intact nAChR, spectra of the transmembrane domain preparation exhibit relatively sharp symmetric amide I band contours centered near 1657 and 1655 cm^{-1} in $^1\text{H}_2\text{O}$ and $^2\text{H}_2\text{O}$, respectively. Both band shapes and frequencies are highly characteristic of α -helical structures. The lack of significant change in band shape upon exposure to $^2\text{H}_2\text{O}$ suggests there is little random coil. The weak intensity near 1635 cm^{-1} in comparison to the intensity observed in spectra of intact nAChR suggests there is minimal if any β -sheet (Figs. 3 and 4).

The strong α -helical character of the nAChR transmembrane domain is supported by a curve-fitting analysis of the amide I contour (data not shown). Curve-fitting suggests an α -helical content of between 75 and 80%, although this value must be viewed as a very rough estimate given the inherent difficulties associated with the curve-fitting complex amide I contours (see “Discussion”). The remaining 20–25% of the peptides adopt structures that vibrate in the 1700–1670 cm^{-1} (β -sheet and/or turn) and 1640–1620 cm^{-1} (β -sheet) regions of the spectra and could reflect the presence of small amounts of transmembrane β -strands. Weak bands in both regions, however, are evident in the spectra of proteins such as myoglobin and bacteriorhodopsin, which are completely devoid of β -sheet (see Fig. 4 and Refs. 28 and 35). The weak bands observed between 1700–1670 cm^{-1} and 1640–1620 cm^{-1} in the transmembrane domain spectra, thus, cannot unequivocally be interpreted in terms of β -sheet in the transmembrane domain.

A quantitative sense of the α -helix and β -sheet character of the transmembrane segments was obtained by comparing the deconvolved spectra with those of proteins of known secondary and tertiary structures (Fig. 4). The deconvolved transmembrane domain spectra contrast sharply those recorded from trypsinogen ($\sim 10\%$ α -helix, $\sim 55\%$ β -sheet) and other proteins, such as the β -barrel membrane protein porin, which exhibits predominantly β -sheet secondary structures (28, 35). Note that

the β -sheet content of trypsinogen approaches that suggested for the nAChR transmembrane domain based on low resolution electron microscopic images. The transmembrane domain spectra are not compatible with the roughly 75% β -sheet content suggested for the nAChR transmembrane domain (17).

The transmembrane domain spectra exhibit much less intensity in both the 1700–1670 cm^{-1} and 1640–1620 cm^{-1} β -sheet regions than is observed in spectra of lysozyme ($\sim 45\%$ α -helix, $\sim 20\%$ β -sheet) and other proteins with low β -sheet content (28). This comparison suggests that much less than 20% of the nAChR transmembrane domain peptides adopt β -sheet secondary structures. A β -sheet content of 10% would only correspond to roughly 1 β -strand/subunit. Given that the length of each hydrophobic segment (M1–M4, 25–30 amino acids) would require the presence of at least 2 or 3 β -strands/subunit (18), the intensities of bands potentially attributable to β -strands may be too low to interpret in terms of any transmembrane β -sheet. The weak bands observed between 1700–1670 cm^{-1} and 1640–1620 cm^{-1} are, thus, likely due to turn or extended structures possibly located in the aqueous environment at the membrane surface as opposed to transmembrane β -strands.

The high α -helical content of the transmembrane domain and the possibility that the non- α -helical amide I vibrations arise from turn and extended structures, both, are supported further by a comparison of the transmembrane domain spectra with those of myoglobin ($\sim 85\%$ α -helix, no β -sheet). Both exhibit relatively narrow and symmetric amide I bands that undergo little change in shape upon exposure to $^2\text{H}_2\text{O}$ [$^1\text{H}/^2\text{H}$ exchange spectra of myoglobin are found in Baenziger and Chew (38)]. The amide I contours are similar in terms of the relative intensities of α -helical and non- α -helical vibrations. The non- α -helical bands also vibrate at similar frequencies. In fact, the only clear difference between the spectra is that the deuterated α -helical structures in myoglobin vibrate at a lower frequency relative to the α -helical structures of the transmembrane domain preparation, which remain predominantly in the protiated form. The latter difference is expected given that α -helical structures, including those of intact nAChR, shift down in frequency by 5–10 cm^{-1} upon complete peptide $^1\text{H}/^2\text{H}$ exchange (11, 12, 30, 38). As noted, protection of the transmembrane domain peptide hydrogens to exchange with deuterium

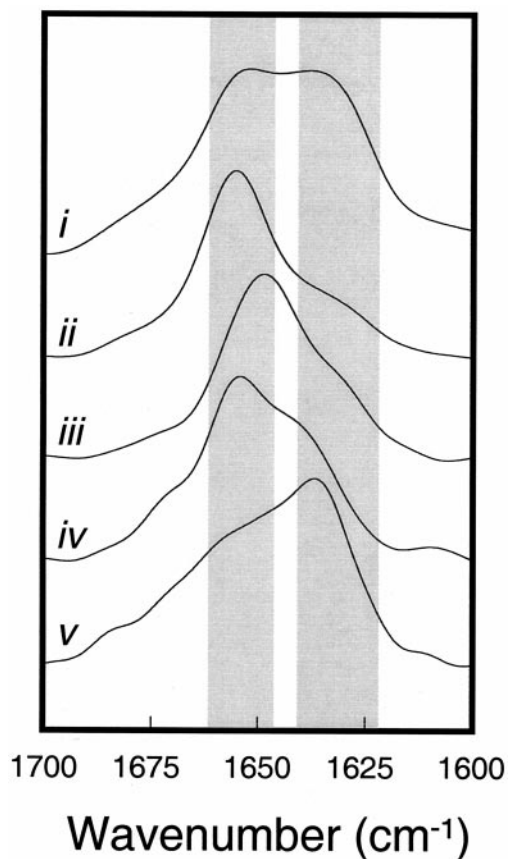


FIG. 4. Comparison of the deconvolved amide I band spectra of intact nAChR, the transmembrane domain, and model proteins. *i*, intact affinity-purified nAChR (~40% α -helix, ~35% β -sheet); *ii*, Pronase-treated transmembrane domain; *iii*, myoglobin (~85% α -helix); *iv*, lysozyme (~45% α -helix, ~20% β -sheet); *v*, trypsinogen (~10% α -helix, ~55% β -sheet). All spectra were recorded in $^2\text{H}_2\text{O}$. The shaded area to the left and right correspond to the frequency regions normally attributed to the α -helix (1660–1648 cm^{-1}) and β -sheet (1640–1620 cm^{-1}) vibrations, respectively. Weak vibrations due to β -sheet and turn structures also vibrate in the 1670–1700 cm^{-1} region. The noted percentages of α -helix and β -sheet were determined by x-ray crystallography for all samples except the intact affinity-purified nAChR. The secondary structure of intact affinity-purified nAChR was estimated by curve-fitting the amide I contour (23). The α -helix and β -sheet content is consistent with the amide I contour shapes of proteins with known secondary structures as discussed in detail in Méthot *et al.* (24). Spectra were deconvolved using Grams/32 version 5.01 with $\gamma = 7.0$ and a Bessel smoothing function set to 80%.

is consistent with a hydrophobic transmembrane location. This spectral comparison shows that both myoglobin and the transmembrane domain preparations have very similar secondary structural contents. In addition, the transmembrane domain amide I band is very similar in terms of the frequencies and relative intensities of both α -helical and non- α -helical component bands to that observed for the α -helical integral membrane protein, bacteriorhodopsin, which also does not exhibit β -sheet (35). The spectra are thus entirely consistent with a transmembrane domain preparation composed predominantly of transmembrane α -helices, the remaining peptides adopting turn or extended structures at the bilayer surface.

Orientation of the Transmembrane Domain—The nAChR transmembrane preparation exhibits dichroic ratios of 2.3 and 1.5 for the amide I and amide II bands, respectively, which both suggest a net orientation preference for α -helices perpendicular to the bilayer surface and contrast the dichroism expected for oriented transmembrane β -strands (Fig. 5) (39). The average net tilt of the transmembrane α -helical polypeptides away from the bilayer normal is $\sim 40^\circ$, although both the mosaic spread of

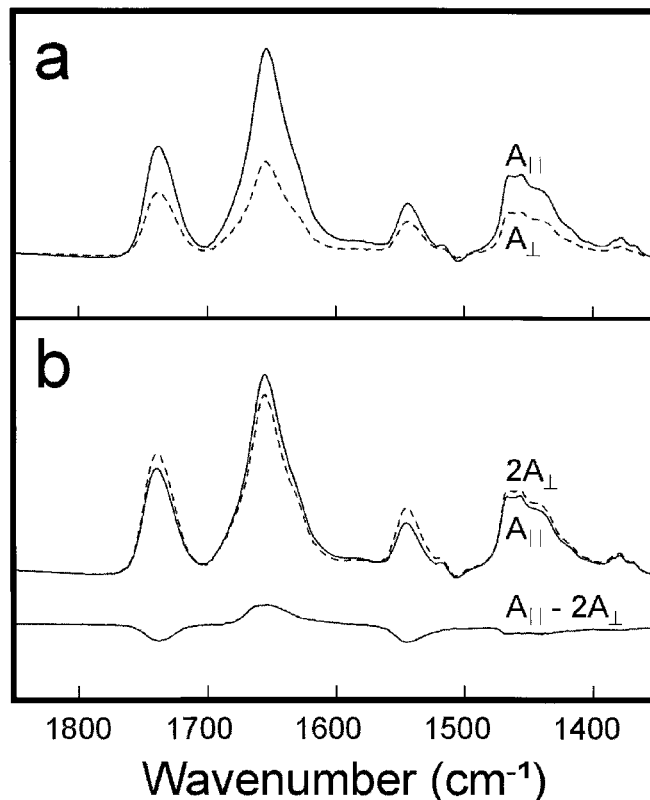


FIG. 5. *a*, spectra of the nAChR transmembrane domain (Pronase-treated) recorded with the infrared light polarized either parallel ($A_{||}$, solid line) or perpendicular (A_{\perp} , dashed line) to the plane of incidence. An R value of 2 corresponds to $R_{\text{isotropic}}$ and usually corresponds to no orientation preference. *b*, the intensity of A_{\perp} has been multiplied by $R_{\text{isotropic}}$ to facilitate comparison, and the difference ($A_{||} - 2A_{\perp}$) was calculated. Positive and negative signals suggest a net orientation either perpendicular or parallel, respectively, to the bilayer normal. Because the amide I and amide II transition dipoles are preferentially oriented parallel and perpendicular to the α -helix long axis, respectively, the dichroism spectra suggest a net orientation of the α -helices perpendicular to the bilayer surface. The orientation of the transmembrane α -helices was calculated according to Hübner and Mantsch (27) from the amide II vibration assuming an angle between the amide II transition dipole and α -helix long axis of either 75 or 90° . These values give net tilts of 38 and 42° , respectively, from the bilayer normal. Note that the measured dichroic ratios for the lipid methylene C-H ($r = 1.7$) and the lipid C=O ($r = 1.7$)-stretching vibrations are closer to $R_{\text{isotropic}}$ than is observed for highly ordered and oriented pure lipid films ($R \sim 1.1$, $R \sim 1.4$, respectively (26)). The consistently larger R values suggest lipid (and, thus, possibly nAChR fragment) motion as well as mosaic spread of the transmembrane containing bilayers (*i.e.* the bilayers are not all perfectly parallel to the germanium surface). Lipid motions are expected given the level of unsaturation in the reconstituted nAChR membranes. Pretreatment of the nAChR membranes with saponin to permeabilize the membranes may increase mosaic spread.

the transmembrane domain-containing bilayers and polypeptide motion average the measured amide I and II band dichroism closer to $R_{\text{isotropic}}$ and, thus, increase the calculated net tilt away from the bilayer normal (see the legend to Fig. 5). The calculated net tilt thus represents a maximum limiting value. The actual net tilt of the transmembrane α -helices is likely much less than 40° .

DISCUSSION

The data presented here suggest an exclusively α -helical structure for the transmembrane domain of the nAChR. This conclusion is based on the highly α -helical character of the infrared spectra recorded from the nAChR transmembrane domain preparations as well as from linear dichroism spectra, which suggest α -helical structures orientated perpendicular to

the bilayer surface. In particular, the amide I contour observed in spectra of the transmembrane domain exhibits much less β -sheet character than spectra of proteins such as lysozyme and trypsinogen, which contain ~20% and ~55% β -sheet content, respectively (28, 35). The transmembrane domain spectrum contrasts sharply that of the β -barrel integral membrane protein, porin (35). Conversely, the transmembrane domain amide I band shape is very similar to the band shapes observed in spectra recorded from myoglobin and the α -helical integral membrane protein bacteriorhodopsin (35), which both lack any β -sheet. These spectral comparisons suggest an almost exclusively α -helical character for the transmembrane domain.

A curve-fitting analysis of the transmembrane domain spectra supports further our conclusion and suggests an α -helical content of 75–80%. Although this value is consistent with the amide I band shape, it should be noted that accurate curve-fitting of complex amide I contours composed of numerous broad overlapping component bands is difficult, particularly when few definitive input parameters (component band shape, height, and width as well as a precise knowledge of the number of bands and base-line position) are available. Although a quantitative analysis of secondary structural content based on amide I band shape comparisons, as performed here, does not provide distinct numerical estimates, the analysis is not affected by the mathematical uncertainties associated with curve-fitting and provides an accurate visual estimate of the relative limits of the α -helix and β -sheet contents. The spectral comparisons noted above show clearly that less than 20% of the nAChR transmembrane peptides adopt a β -sheet structure, assuming that all bands in non- α -helical regions of the spectra are due to β structures. Note that 10% β -sheet content is not sufficient to account for the 2–3 transmembrane β -strands required to account for one transmembrane segment of 25–30 amino acids in each subunit. Conversely, the close similarity between the amide I band shapes in spectra of the transmembrane domain and myoglobin suggests similar secondary structures for these two proteins and is, thus, consistent with a transmembrane domain preparation composed of at least 80% α -helix with the remaining peptides adopting extended or turn structures. Given that the studied transmembrane fragments are 3–6 kDa in length, the most plausible interpretation of our data is that the transmembrane domain preparation is composed of α -helical transmembrane structures with extended or turn structures at the bilayer surface.

This conclusion contrasts a recent study of the transmembrane domain of the nAChR generated after proteolytic treatment of native nAChR membranes (18). The latter study calculated a secondary structural content of ~50% α -helix, ~40% β -structure and turn and 10% random and concluded a mixed α -helix/ β -sheet transmembrane domain. The discrepancy between the two studies can be attributed to a number of factors. First, the native membrane preparations used in the latter may contain non-nAChR impurities, such as a *Torpedo* analog of the voltage-dependent transmembrane anion channel (40). This protein shares homology with the β -barrel porins, and its possible presence in the native transmembrane preparations could contribute to the β -sheet character of the spectra. Second, the presented secondary structural analysis of Gorne-Tschelnokow *et al.* (18) was performed on spectra recorded in $^1\text{H}_2\text{O}$. Because $^1\text{H}_2\text{O}$ vibrations overlap the amide I band in a region normally attributed to β -sheet, unavoidable difficulties subtracting $^1\text{H}_2\text{O}$ from the spectra could have contributed to the calculated β -sheet content of the transmembrane domain. Finally, the analysis of Gorne-Tschelnokow *et al.* (18) did not take into

account the possibility that weak non- β -sheet vibrations can occur in regions of FTIR spectra normally attributed to β -sheet, as has been observed in spectra of numerous α -helical proteins (Fig. 4 and Refs. 28 and 35). Although the relative merits of assigning such weak bands to β -sheet *versus* turn and/or extended structures is debatable, it is significant to note that the β -sheet content suggested by Gorne-Tschelnokow *et al.* for the transmembrane domain is similar to that which has been reported for intact nAChR despite dramatically different amide I band shapes for the intact and proteolyzed receptor. Furthermore, the amide I band shapes observed for the transmembrane domain both here and in the work of Gorne-Tschelnokow *et al.* (18) do not exhibit close to the same level of β -sheet character that is observed in spectra of other proteins that contain 30–40% β -sheet. These empirical comparisons, which are at the heart of all FTIR analyses of protein secondary structure (although supported by theoretical calculations), indicate that the nAChR transmembrane domain does not contain a large percentage of transmembrane β -sheet.

In conclusion, although we cannot completely rule out the possibility, there is no definitive evidence in our spectra for the existence of any β -sheet in the transmembrane domain preparations of the nAChR. The strong α -helical character of the nAChR transmembrane segments is consistent with biophysical studies of individual transmembrane segments (13–16) and both chemical labeling and hydrogen-deuterium exchange studies of intact nAChR (8–12), although M1 may form a distorted α -helix (36, 37). Our results strongly suggest that the transmembrane domain of the nAChR and likely other members of the ligand-gated ion channel superfamily is formed from five bundles of four transmembrane α -helices.

Acknowledgment—We thank Dan Kaiser for preparing the figures.

REFERENCES

- Smith, G. B. & Olsen, R. W. (1995) *Trends Pharmacol. Sci.* **16**, 162–168
- Jackson, M. B. & Yakel, J. L. (1995) *Annu. Rev. Physiol.* **57**, 447–468
- Kuhse, J., Betz, H. & Kirsch, J. (1995) *Curr. Opin. Neurobiol.* **5**, 318–323
- Changeux, J. P. & Edelman, S. J. (1998) *Neuron* **21**, 959–980
- Noda, M., Takahashi, H., Tanabe, T., Toyosato, M., Kikuyotani, S., Furutani, Y., Hirose, T., Takashima, H., Inayama, S., Miyata, T. & Numa, S. (1983) *Nature* **302**, 528–532
- Claudio, T., Ballivet, M., Patrick, J. & Heinemann, S. (1983) *Proc. Natl. Acad. Sci. U. S. A.* **80**, 1111–1115
- Revah, F., Galzi, J. L., Giraudat, J., Haumont P. Y., Lederer, F. & Changeux, J. P. (1990) *Proc. Natl. Acad. Sci. U. S. A.* **87**, 4675–4679
- Blanton, M. P. & Cohen, J. B. (1994) *Biochemistry* **33**, 2859–2872
- Blanton, M. P. & Cohen, J. B. (1992) *Biochemistry* **31**, 3738–3750
- Tamamizu, S., Guzman, G. R., Santiago, J., Rojas, L. V., McNamee, M. G. & Lasalde-Dominicci, J. A. (2000) *Biochemistry* **39**, 4666–4673
- Baenziger, J. E. & Méthot, N. (1995) *J. Biol. Chem.* **270**, 29129–29137
- Méthot, N. & Baenziger, J. E. (1998) *Biochemistry* **37**, 14815–14822
- Corbin, J., Méthot, N., Wang, H. H., Baenziger, J. E. & Blanton, M. P. (1998) *J. Biol. Chem.* **273**, 771–777
- Opella, S. J., Marassi, F. M., Gesell, J. J., Valente, A. P., Kim, Y., Oblatt-Montal, M. & Montal, M. (1999) *Nat. Struct. Biol.* **6**, 374–379
- Lugovskoy, A. A., Maslennikov, I. V., Utkin, Y. N., Tsetlin, V. I., Cohen, J. B. & Arseniev, A. S. (1998) *Eur. J. Biochem.* **255**, 455–461
- Pashkov, V. S., Maslennikov, I. V., Tchikin, L. D., Efremov, R. G., Ivanov, V. T. & Arseniev, A. S. (1999) *FEBS Lett.* **457**, 117–121
- Unwin, N. (1993) *J. Mol. Biol.* **229**, 1101–1124
- Gorne-Tschelnokow, U., Strecker, A., Kaduk, C., Naumann, D. & Hucho, F. (1994) *EMBO J.* **13**, 338–341
- Hucho, F., Gorne-Tschelnokow, U. & Strecker, A. (1994) *Trends Biochem. Sci.* **19**, 383–387
- Ortells, M. O. & Lunt, G. G. (1996) *Protein Eng.* **9**, 51–59
- Leite, J. F., Amosato, A. A. & Cascio, M. (2000) *J. Biol. Chem.* **275**, 13683–13689
- Cascio, M., Shenkel, S., Grodzicki, R. L., Sigworth, F. J. & Fox, R. O. (2001) *J. Biol. Chem.* **276**, 20981–20988
- McCarthy, M. P. & Moore, M. A. (1992) *J. Biol. Chem.* **267**, 7655–7663
- Méthot, N., McCarthy, M. P. & Baenziger, J. E. (1994) *Biochemistry* **33**, 7709–7717
- Shägger, H. & von Jagow, G. (1987) *Anal. Biochem.* **166**, 368–379
- Günthard, H. H. (1981) in *Membrane Spectroscopy* (Grell, E., ed) pp. 270–332, Springer-Verlag, Berlin
- Hübner, W. & Mantsch, H. H. (1991) *Biophys. J.* **59**, 1261–1272
- Byler, D. M. & Susi, H. (1986) *Biopolymers* **25**, 469–487
- Jackson, M. & Mantsch, H. H. (1995) *Crit. Rev. Biochem. Mol. Biol.* **30**, 95–120

30. Tamm, L. K. & Tatulian, S. A. (1997) *Q. Rev. Biophys.* **30**, 365–429
31. Dousseau, F. & Pézolet, M. (1990) *Biochemistry* **29**, 8771–8779
32. Naumann, D., Schultz, C., Gorne-Tschelnokow, U. & Hucho, F. (1993) *Biochemistry* **32**, 3162–3168
33. Brunner, J. (1993) *Annu. Rev. Biochem.* **62**, 483–514
34. Noda, M., Takahashi, H., Tanabe, T., Toyosato, M., Furutani, Y., Hirose, T., Asai, M., Inayama, S., Miyata, T. & Numa, S. (1982) *Nature* **299**, 793–797
35. Goormaghtigh, E., Cabiliax, V. & Ruysschaert, J. M. (1990) *Eur. J. Biochem.* **193**, 409–420
36. Akabas, M. H. & Karlin, A. (1995) *Biochemistry* **34**, 12496–12500
37. Barrantes, F. J., Antollini, S. S., Blanton, M. P. & Prieto, M. (2000) *J. Biol. Chem.* **275**, 37333–37339
38. Baenziger, J. E. & Chew, J. (1997) *Biochemistry* **36**, 3617–3624
39. Marsh, D. (1997) *Biophys. J.* **72**, 2710–2718
40. Blanton, M. P., Lala, A. K. & Cohen, J. B. (2001) *Biochim. Biophys. Acta*, in press